

- (2) Claus, C. *Justus Liebigs Ann. Chem.* **1846**, *59*, 283.  
 (3) Adamson, M. G. *Aust. J. Chem.* **1967**, *20*, 2517.  
 (4) Adamson, M. G. *J. Chem. Soc. A* **1968**, 1370.  
 (5) Rose, D.; Wilkinson, G. J. *J. Chem. Soc. A* **1970**, 1791.  
 (6) Mercer, E. E.; Dumas, P. E. *Inorg. Chem.* **1971**, *10*, 2755.  
 (7) Howe, J. L. *J. Am. Chem. Soc.* **1901**, *23*, 781.  
 (8) Godward, L. W. N.; Wardlaw, W. J. *J. Chem. Soc.* **1938**, 1422.  
 (9) Stephenson, T. A.; Wilkinson, G. J. *Inorg. Nucl. Chem.* **1966**, *28*, 2285.  
 (10) Cotton, F. A.; Frenz, B. A.; Deganello, G.; Shaver, A. J. *Organomet. Chem.* **1973**, *50*, 227. Adams, R. D.; Collins, D. M.; Cotton, F. A. *J. Am. Chem. Soc.* **1974**, *96*, 749.  
 (11) All crystallographic computing was done on a PDP 11/45 computer at the Molecular Structure Corp., College Station, Texas, using the Enraf-Nonius structure determination package.  
 (12) Williams, J. M.; Peterson, S. W.; Levy, H. A. Abstracts, ACA Winter Meeting, 1972, p 51.  
 (13) Lundgren, J.-O.; Olovsson, I. "The Hydrogen Bond—Recent Developments in Theory and Experiment", Schuster, P., Ed.; North-Holland Publishing Co.: Amsterdam, 1976.  
 (14) Cotton, F. A.; Ucko, D. A. *Inorg. Chim. Acta* **1972**, *6*, 161.  
 (15) Delphin, W. H.; Wentworth, R. A. D.; Matson, M. S. *Inorg. Chem.* **1974**, *13*, 2553.

## Cytochrome Oxidase Models. 2. $\mu$ -Bipyrimidyl Mixed-Metal Complexes as Synthetic Models for the Fe/Cu Binuclear Active Site of Cytochrome Oxidase<sup>1</sup>

Randall H. Petty,<sup>2a</sup> Byron R. Welch,<sup>2a</sup> Lon J. Wilson,\*<sup>2a,3</sup>  
 Lawrence A. Bottomley,<sup>2b</sup> and Karl M. Kadish\*<sup>2b</sup>

Contribution from the Department of Chemistry, William Marsh Rice University, Houston, Texas 77001, and the Department of Chemistry, University of Houston, Houston, Texas 77004. Received April 13, 1979

**Abstract:**  $\mu$ -Bipyrimidyl (bipym) mixed-metal complexes, with  $[\text{Fe}^{\text{II}}(\text{bipym})\text{M}^{\text{II}}]$  cores ( $\text{M}^{\text{II}} = \text{Cu}$  and  $\text{Zn}$ ), have been synthesized to model the proposed imidazole-bridged  $[\text{Cyt } a_3^{3+}(\text{imid})\text{Cu}_2^{2+}]$  active site structure of cytochrome oxidase where  $-J(\text{Fe}^{\text{II}}-\text{Cu}^{\text{II}}) \geq 200 \text{ cm}^{-1}$ . The binuclear compounds have been prepared from a six-coordinate  $[\text{Fe}^{\text{II}}(\text{C}_{18}\text{H}_{18}\text{N}_6)(\text{bipym})]^{2+}$  species (B) ( $\text{C}_{18}\text{H}_{18}\text{N}_6 =$  a folded macrocycle) by reaction with the appropriate bis(acetylacetonato)M(II) compound in  $\text{CH}_2\text{Cl}_2$  to yield  $[\text{Fe}^{\text{II}}(\text{C}_{18}\text{H}_{18}\text{N}_6)(\text{bipym})\text{Cu}^{\text{II}}(\text{acac})_2]^{2+}$  (C) and  $[\text{Fe}^{\text{II}}(\text{C}_{18}\text{H}_{18}\text{N}_6)(\text{bipym})\text{Zn}^{\text{II}}(\text{acac})_2]^{2+}$  (D) as  $\text{ClO}_4^-$  salts. Compound B contains low-spin iron(II), whereas C and D are high-spin species in both the solid and solution states at room temperature. Comparative variable-temperature (10–300 K) magnetic susceptibility measurements for C and D indicate C to contain magnetically isolated  $S = 2$  ( $\text{Fe}^{\text{II}}$ ) and  $S = 1/2$  ( $\text{Cu}^{\text{II}}$ ) centers with  $J \approx 0$  through the bipym bridge. In the  $^{57}\text{Fe}$  Mössbauer spectra of C and D and the  $\text{Cu}^{\text{II}}$  EPR spectrum of C at 8 K are also supportive of this interpretation. In solution, the redox activity of B, C, and D has been examined by cyclic voltammetry in  $\text{CH}_2\text{Cl}_2$  where  $E_{1/2}$  for the  $\text{Fe}^{\text{II}}/\text{Fe}^{\text{III}}$  couple of high-spin C and D are identical at +0.60 V (SCE) and 700 mV lower in potential than for the low-spin monomer compound (B). The  $\text{Cu}^{\text{II}}/\text{Cu}^{\text{I}}$  couple for C appears to occur at  $E_{1/2} = -0.24 \text{ V}$  (SCE). Finally, the  $\mu$ -bipyrimidyl  $\text{Cu}_2$  compound,  $[(\text{hfa})_2\text{Cu}^{\text{II}}(\text{bipym})\text{Cu}^{\text{II}}(\text{hfa})_2]$  ( $\text{hfa}^- =$  hexafluoroacetylacetonato anion), has been prepared and found to exhibit an antiferromagnetic exchange interaction with  $-J = 7.9 \text{ cm}^{-1}$ . The ramifications of these results as they pertain to the magnetically coupled  $[\text{Cyt } a_3^{3+}-\text{Cu}_2^{2+}]$  active site of resting cytochrome oxidase are discussed, and an oxo-bridged alternative to the imidazole-bridge possibility is also considered in view of the findings from the present model study.

### Introduction

One of the most complex and enigmatic of metalloenzymes is cytochrome oxidase, the terminal oxidation/reduction enzyme in mitochondrial respiration. The enzyme catalytically reduces 1 mol of molecular oxygen to 2 mol of water, with the concomitant release of energy which is stored in the ADP-ATP cycle.<sup>4</sup> The protein contains four metal centers (two irons and two coppers) per functioning enzyme unit.<sup>5</sup> Furthermore, through various spectroscopic (EPR, MCD, and UV-vis) and other studies, it is now known that the enzyme contains one isolated iron heme unit (cytochrome *a*) which is low spin in both the oxidized and reduced forms and one isolated copper center ( $\text{Cu}_D$ ; D for EPR detectable), while at the active or oxygen binding site there is a high-spin iron heme (cytochrome  $a_3$ ) and a second copper center ( $\text{Cu}_U$ ; U for EPR undetectable).<sup>6,7</sup> In a full-temperature magnetochemical study, we have recently shown for the fully oxidized or resting form of the protein that the iron centers of  $\text{Cyt } a_3^{3+}$  and  $\text{Cu}_U^{2+}$  are strongly coupled antiferromagnetically ( $-J \geq 200 \text{ cm}^{-1}$ ) through a bridge which was suggested to be imidazolate (imid) from a histidine residue.<sup>8,9</sup> This proposed structure for the active site is shown schematically in Figure 1. The observed "strong" magnetic exchange interaction for oxidase is also manifested in the EPR spectrum, where there appears only one

$g = 2$  signal which is assigned to magnetically isolated  $\text{Cu}_D$  and quantitates to only approximately 40% of the total copper present.<sup>10</sup> This information, in conjunction with the magnetic susceptibility data, appears to rule out any other possible combinations of metal spin-state and exchange interaction as highly unlikely.<sup>8</sup> It does not, however, contribute any information concerning the nature of the possible bridge which mediates the exchange between the iron and copper centers. However, there are two pieces of circumstantial evidence that point to imidazolate as the bridge: (1) EPR measurements indicate that the iron center of the  $a_3$  heme has a nitrogen atom as one of its apical donor atoms<sup>11</sup> and (2) superoxide dismutase, for which a crystal structure is available, contains a mixed-metal binuclear  $[\text{Cu}^{\text{II}}(\text{imid})\text{Zn}^{\text{II}}]$  site with an imidazolate bridge from histidine.<sup>12,13</sup>

There are now several examples of synthetic complexes which contain imidazolate-bridged metal centers.<sup>14–18</sup> Thus, there is no question of the bridging capabilities of the imidazolate anion. The controversy that has arisen is over the ability of imidazolate to foster an exchange of the magnitude ( $-J \geq 200 \text{ cm}^{-1}$ ) present for the  $[\text{Fe}^{\text{II}}-\text{Cu}^{\text{II}}]$  pair of cytochrome oxidase.<sup>8,14,18</sup> For a derivative of superoxide dismutase, with the  $\text{Zn}^{\text{II}}$  ion replaced by a second  $\text{Cu}^{\text{II}}$ , the strength of the antiferromagnetic exchange between the two  $\text{Cu}^{\text{II}}$  centers is

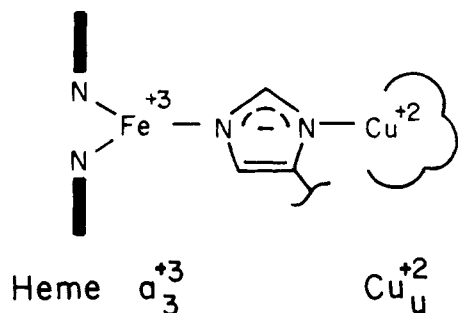


Figure 1. Schematic of the proposed imidazolite-bridged structure for the active site of resting cytochrome oxidase.

only  $26\text{ cm}^{-1}$ .<sup>13</sup> Furthermore, all other examples of synthetic  $[\text{Cu}^{\text{II}}(\text{imid})\text{Cu}^{\text{II}}]$  and related systems exhibit antiferromagnetic exchange interactions in the  $0\text{--}90\text{-cm}^{-1}$  range,<sup>14–18</sup> or far less than the  $200\text{-cm}^{-1}$  value displayed by oxidase. To date, there has been only one measurement on a mixed-metal binuclear complex in which the bridging ligand is known to be imidazolite, where a  $\text{Co}^{\text{II}}$  substituted derivative of superoxide dismutase appears to be a case of strong exchange between a  $[\text{Cu}^{\text{II}}(\text{imid})\text{Co}^{\text{II}}]$  pair with  $-J \geq 300\text{ cm}^{-1}$ .<sup>19</sup>

The construction of synthetic model compounds represents one of the most viable approaches toward testing the proposed structure for the oxidase active site as shown in Figure 1. At present, however, there are no known examples of such synthetic, mixed-metal binuclear complexes with imidazolite bridges.<sup>20a</sup> In fact, very few binuclear complexes containing different transition metals have been reported,<sup>20b</sup> and there appears to be only one authenticated example of a synthetic  $[\text{Fe}-(\text{B})-\text{Cu}]$  complex with a direct ligand bridge of any nature.<sup>20c</sup> Toward systematically producing such compounds to model cytochrome oxidase, we recently communicated<sup>21</sup> initial results reporting the first N-heterocyclic-bridged  $[\text{Fe}-(\text{B})-\text{Cu}]$  species to be isolated where  $\text{B} = 2,2'$ -bipyrimidine (bipym). The present work reports an extended investigation of this study which further comments on the likelihood of a  $[\text{Cyt } a_3(\text{imid})\text{Cu}_U]$  structure for the active site of cytochrome oxidase. Finally, an alternative  $\text{O}_2$ -bridged model for the site is also considered in light of the information obtained by this initial modeling study.

## Experimental Section

**Physical Measurements.** Variable-temperature magnetic susceptibility measurements in the solid state were performed by the Faraday technique using equipment previously described.<sup>22</sup> Solution magnetic susceptibilities were performed by Evans' method<sup>23</sup> on a Varian EM-390 NMR spectrometer. Pascal's constants were used to correct for ligand and anion diamagnetism in cgsu for 2,2'-bipyrimidine,  $-96.3 \times 10^{-6}$ ;  $\text{acac}^-$ ,  $-55 \times 10^{-6}$ ;  $\text{hfac}$ ,  $-70.2 \times 10^{-6}$ ;  $\text{C}_{18}\text{H}_{18}\text{N}_6$ ,  $-203.2 \times 10^{-6}$ ;  $\text{ClO}_4^-$ ,  $-32 \times 10^{-6}$ .

Mössbauer spectra were obtained using a previously described spectrometer and computer analyzed by the program of Chrisman and Tumolillo.<sup>24</sup> Temperatures were monitored by a copper vs. constantan thermocouple imbedded in the sample. Computer-generated plots of the Mössbauer spectra were obtained using a Calcomp plotting program.

Osmometry measurements were obtained using an HP 302 B vapor pressure osmometer. Solution conductivities were measured on a Model 31 YSI conductivity bridge. UV-vis spectra were obtained on a Cary 17 recording spectrometer using quartz cells.

X-Band EPR spectra were obtained as  $\text{CH}_2\text{Cl}_2$  glasses on a Varian E-line EPR spectrometer using standard quartz cells. Field positions were referenced relative to DPPH; the copper content of the samples was quantified by computer signal integration using known concentrations of  $\text{CuSO}_4$  as standards.

Electrochemical measurements were obtained in  $\text{CH}_2\text{Cl}_2$  and  $\text{CH}_3\text{CN}$  at room temperature using an EG & G PAR Model 173 potentiostat/galvanostat driven by a Model 175 universal programmer

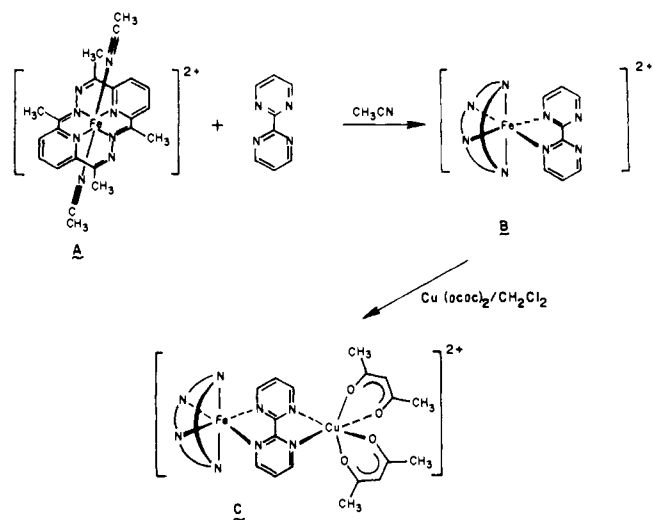


Figure 2. Synthetic scheme for the preparation of the mononuclear (B) and binuclear  $[\text{Fe}^{\text{II}}(\text{bipym})\text{Cu}^{\text{II}}]$  (C) iron(II) complexes. (Compound D in the text is the corresponding  $[\text{Fe}^{\text{II}}(\text{bipym})\text{Zn}^{\text{II}}]$  derivative.)

or a Model 174 A polarographic analyzer. The current/voltage curves were recorded on a Houston Omnigraphic 2000 X-Y recorder at scan rates between  $0.02$  and  $0.50\text{ V/s}$  and a Tektronix Model 5111 storage oscilloscope at scan rates between  $0.10$  and  $50.0\text{ V/s}$ . A three-electrode geometry was employed; a platinum button served as the working electrode for cyclic voltammetric studies and a dropping mercury electrode (DME) for polarographic studies, a platinum wire as the counter electrode, and a Metrohm K901 saturated calomel electrode (SCE) as the reference electrode. The reference electrode was partially separated from the bulk solution by means of a fritted-glass bridge containing supporting electrolyte solution. All solutions were  $10^{-3}\text{ M}$  in the complex and  $0.1\text{ M}$  in tetrabutylammonium perchlorate (TBAP) as the supporting electrolyte.

Chemical analyses were performed by the microanalytical laboratory of the School of Chemical Sciences, University of Illinois.

**Materials and Syntheses.** 2,6-Diacetylpyridine, hydrazine, 2-aminopyrimidine, acetylacetone, and hexafluoroacetylacetone were obtained from Aldrich Chemical Co. and used without further purification. All solvents used in syntheses were reagent grade and spectroquality for the spectral measurements.

**2-Bromopyrimidine** was prepared from 2-aminopyrimidine by the method of Bly and Mellon<sup>25</sup> and purified by sublimation.

**2,2'-Bipyrimidine (bipym)** was prepared by the coupling of 2-bromopyrimidine in the presence of a copper-bronze catalyst. Equal weights of 2-bromopyrimidine and the copper-bronze catalyst were thoroughly mixed and sealed in an evacuated flask. After reaction at  $110^\circ\text{C}$  for 12 h, the flask was opened and the products were worked up according to the procedure of Bly and Mellon<sup>25</sup> and Westcott.<sup>26</sup> The final product was purified by sublimation at  $95^\circ\text{C}$  ( $1\text{ mmHg}$ ); yields varied from 10 to 20%; mp  $110\text{--}113^\circ\text{C}$ ; mass spectrum  $\text{M}^+ 158$ .

$[\text{Fe}^{\text{II}}(\text{C}_{18}\text{H}_{18}\text{N}_6)(\text{CH}_3\text{CN})_2](\text{ClO}_4)_2$  was prepared by the procedure of Goedkin et al.<sup>27</sup> The compound was recrystallized from  $\text{CH}_3\text{CN}$  and  $\text{EtOH}$ , washed with  $\text{EtOH}$  and  $\text{Et}_2\text{O}$ , and dried over  $\text{P}_2\text{O}_5$  in vacuo at room temperature. Anal. Calcd for  $\text{FeC}_{22}\text{H}_{24}\text{N}_8\text{Cl}_2\text{O}_8$ : C, 40.32; H, 3.69; N, 17.10; Fe, 8.52. Found: C, 40.02; H, 3.69; N, 16.90; Fe, 8.79.

$[\text{Fe}^{\text{II}}(\text{C}_{18}\text{H}_{18}\text{N}_6)(\text{bipym})](\text{ClO}_4)_2$  was prepared by the addition of  $0.1\text{ mmol}$  of  $[\text{Fe}^{\text{II}}(\text{C}_{18}\text{H}_{18}\text{N}_6)(\text{CH}_3\text{CN})_2](\text{ClO}_4)_2$  dissolved in a minimum amount of warm  $\text{CH}_3\text{CN}$  to  $0.1\text{ mmol}$  of 2,2'-bipyrimidine dissolved in  $10\text{ mL}$  of  $\text{CH}_3\text{CN}$ . The solution immediately changed from blue-green to red upon mixing. The  $\text{CH}_3\text{CN}$  was removed under reduced pressure at room temperature to yield a red solid which was recrystallized from a  $\text{CH}_2\text{Cl}_2$ /heptane mixture. The resulting red crystals were collected by filtration and dried over  $\text{P}_2\text{O}_5$  in vacuo at room temperature for 12 h. Anal. Calcd for  $\text{FeC}_{26}\text{H}_{24}\text{N}_{10}\text{Cl}_2\text{O}_8 \cdot \text{CH}_2\text{Cl}_2$ : C, 39.76; H, 3.21; N, 17.17; Fe, 6.84. Found: C, 40.09; H, 3.37; N, 17.18; Fe, 6.76.

$[\text{Fe}^{\text{II}}(\text{C}_{18}\text{H}_{18}\text{N}_6)(\text{bipym})\text{M}^{\text{II}}(\text{acac})_2](\text{ClO}_4)_2$ , where  $\text{M}^{\text{II}} = \text{Cu}$  or  $\text{Zn}$ , was prepared by the addition of  $0.1\text{ mmol}$  of  $[\text{M}^{\text{II}}(\text{acac})_2]$  to a solution containing  $0.1\text{ mmol}$  of  $[\text{Fe}^{\text{II}}(\text{C}_{18}\text{H}_{18}\text{N}_6)(\text{bipym})](\text{ClO}_4)_2$  dissolved

in  $\text{CH}_2\text{Cl}_2$ . The solution changed from red to purple upon mixing. The solvent was removed in vacuo at room temperature and the purple solid recrystallized from a  $\text{CH}_2\text{Cl}_2$ /heptane mixture. The resulting purple crystals were collected by filtration and dried over  $\text{P}_2\text{O}_5$  in vacuo at room temperature for 12 h. Anal. Calcd for  $\text{FeCuC}_{36}\text{H}_{38}\text{N}_{10}\text{O}_{12}\text{Cl}_2 \cdot 0.5\text{CH}_2\text{Cl}_2$ : C, 42.34; H, 3.80; N, 13.58; Fe, 5.39; Cu, 6.14. Found: C, 42.58; H, 4.00; N, 13.42; Fe, 5.63; Cu, 6.16. Anal. Calcd for  $\text{FeZnCuC}_{36}\text{H}_{38}\text{N}_{10}\text{O}_{12}\text{Cl}_2 \cdot 0.5\text{C}_7\text{H}_{16}$ : C, 45.40; H, 4.45; N, 13.34; Fe, 5.31; Zn, 6.22. Found: C, 45.23; H, 4.38; N, 13.54; Fe, 5.53; Zn, 6.34.

$[(\text{hfa})_2\text{Cu}^{\text{II}}(\text{bipym})\text{Cu}^{\text{II}}(\text{hfa})_2]$  was prepared by the addition of 0.2 mmol of  $[\text{Cu}(\text{hfac})_2(\text{H}_2\text{O})]$  dissolved in 25 mL of  $\text{CH}_2\text{Cl}_2$  to 0.1 mmol of 2,2'-bipyrimidine also dissolved in 25 mL of  $\text{CH}_2\text{Cl}_2$ . The solvent was removed in vacuo at room temperature and the light green solid was recrystallized from  $\text{Et}_2\text{O}$ . The resulting light green crystals were collected by filtration and dried over  $\text{P}_2\text{O}_5$  in vacuo at room temperature for 12 h. Anal. Calcd for  $\text{Cu}_2\text{C}_{28}\text{H}_{10}\text{N}_4\text{O}_8\text{F}_{24} \cdot 0.5(\text{C}_2\text{H}_5)_2\text{O}$ : C, 25.06; H, 1.43; N, 5.31; Cu, 12.05. Found: C, 25.20; H, 1.28; N, 5.11; Cu, 11.10. Mol wt in chloroform by osmometry: theoretical, 1017; found, 1090.

## Results and Discussion

### Synthesis and Characterization of the Complexes in Solution.

Synthesis of the green macrocyclic  $[\text{Fe}^{\text{II}}(\text{C}_{18}\text{H}_{18}\text{N}_6)(\text{CH}_3\text{CN})_2]^{2+}$  complex, A in Figure 2, involves a Schiff-base condensation of 2,6-diacetylpyridine with hydrazine, as first described by Goedkin et al.<sup>27</sup> The macrocyclic ligand is of special interest here in that with axial  $\text{CH}_3\text{CN}$  ligands the macrocycle is planar, while with strong-field, bidentate ligands such as 2,2'-bipyridine<sup>27</sup> [or in this study, 2,2'-bipyrimidine (bipym)] the macrocycle "folds" to accommodate the bidentate ligand as shown by B in Figure 2. Thus, when bipym is added to a  $\text{CH}_3\text{CN}$  solution containing  $[\text{Fe}^{\text{II}}(\text{C}_{18}\text{H}_{18}\text{N}_6)(\text{CH}_3\text{CN})_2](\text{ClO}_4)_2$ , a red, crystalline solid is isolated which has been characterized as the mononuclear  $[\text{Fe}^{\text{II}}(\text{C}_{18}\text{H}_{18}\text{N}_6)(\text{bipym})](\text{ClO}_4)_2$  species. Further reaction of the  $[\text{Fe}^{\text{II}}(\text{C}_{18}\text{H}_{18}\text{N}_6)(\text{bipym})]^{2+}$  cation with  $[\text{Cu}^{\text{II}}(\text{acac})_2]$  in a noncoordinating solvent such as  $\text{CH}_2\text{Cl}_2$  yields a purple, microcrystalline product which has been characterized as the  $\mu$ -bipyrimidyl species,  $[\text{Fe}^{\text{II}}(\text{C}_{18}\text{H}_{18}\text{N}_6)(\text{bipym})\text{Cu}^{\text{II}}(\text{acac})_2](\text{ClO}_4)_2$  (C). Substitution of  $[\text{Zn}^{\text{II}}(\text{acac})_2]$  in the reaction yields the corresponding  $[\text{Fe}^{\text{II}}(\text{bipym})\text{Zn}^{\text{II}}]$  analogue, D. Compounds C and D are the first  $\mu$ -bipyrimidyl mixed-metal species to be reported, although pure-metal binuclear complexes of  $\text{Pt}_2$  and  $\text{Ru}_2$  are known.<sup>28-30</sup> Both of the mixed-metal compounds are soluble and stable in noncoordinating solvents such as  $\text{CH}_2\text{Cl}_2$  or  $\text{CHCl}_3$  for short periods of time (1 h); however, in  $\text{CH}_3\text{CN}$ , the binuclear complexes dissociate into the original  $[\text{Fe}^{\text{II}}(\text{C}_{18}\text{H}_{18}\text{N}_6)(\text{CH}_3\text{CN})_2]^{2+}$  species and  $[\text{Cu}^{\text{II}}(\text{acac})_2]$  or  $[\text{Zn}^{\text{II}}(\text{acac})_2]$ . For this reason solvent studies in the present work have been largely limited to  $\text{CH}_2\text{Cl}_2$ . Attempts to isolate a mononuclear  $[\text{Cu}^{\text{II}}(\text{acac})_2(\text{bipym})]$  complex were unsuccessful, indicating that the nitrogen atoms of free base bipym are less basic than the backside, uncoordinated nitrogens of the  $[\text{Fe}^{\text{II}}(\text{C}_{18}\text{H}_{18}\text{N}_6)(\text{bipym})]^{2+}$  complex. When complexes with "more acidic" copper centers, such as  $[\text{Cu}^{\text{II}}(\text{hfac})_2]$  ( $\text{hfac}^- = \text{hexafluoroacetylacetonate anion}$ ), are reacted with B, the bipym ligand is stripped from the iron center and the resulting  $[\text{Cu}^{\text{II}}(\text{hfac})_2(\text{bipym})]$  complex can be isolated. Although no bipym adduct of  $[\text{Cu}^{\text{II}}(\text{acac})_2]$  could be isolated, both mononuclear and binuclear complexes of  $[\text{Cu}^{\text{II}}(\text{hfac})_2]$  are obtainable. The binuclear  $[(\text{hfac})_2\text{Cu}^{\text{II}}(\text{bipym})\text{Cu}^{\text{II}}(\text{hfac})_2]$  complex is of special interest in the present work and is discussed more fully below.

Electronic absorption spectra of the complexes have been obtained in solution for purposes of comparison and to completely characterize the species. The spectra are shown in Figure 3 with band positions and intensities summarized in Table I. Owing to their intensities, all of the observed bands are most reasonably assigned to charge-transfer transitions, and a careful search at lower energy failed to resolve any low

**Table I.** Electronic Spectral Data for Complexes in Solution

complex	$\lambda_{\text{max}}$ , nm <sup>a</sup>	$\epsilon$ , M <sup>-1</sup> cm <sup>-1</sup> <sup>a</sup>
$[\text{Fe}^{\text{II}}(\text{C}_{18}\text{H}_{18}\text{N}_6)(\text{CH}_3\text{CN})_2](\text{ClO}_4)_2$ <sup>b</sup>	380	3180
	565	1400
	640	1840
	695	2700
	770	2880
$[\text{Fe}^{\text{II}}(\text{C}_{18}\text{H}_{18}\text{N}_6)(\text{bipym})](\text{ClO}_4)_2$ <sup>c</sup>	440	3700
	470	3600
	540	3780
	740	480
$[\text{Fe}^{\text{II}}(\text{C}_{18}\text{H}_{18}\text{N}_6)(\text{bipym})\text{Cu}^{\text{II}}(\text{acac})_2](\text{ClO}_4)_2$ <sup>c</sup>	550	3870
	725	2220
$[\text{Fe}^{\text{II}}(\text{C}_{18}\text{H}_{18}\text{N}_6)(\text{bipym})\text{Zn}^{\text{II}}(\text{acac})_2](\text{ClO}_4)_2$ <sup>c</sup>	550	1870
	735	1290

<sup>a</sup> Band positions and intensities have been estimated without deconvolution procedures. <sup>b</sup>  $\text{CH}_3\text{CN}$  solution. <sup>c</sup>  $\text{CH}_2\text{Cl}_2$  solution.

intensity bands which could be assigned as purely "d-d" in nature. Such "d-d" bands have only rarely been detected for six-coordinate  $\text{Fe}^{\text{II}}$  complexes containing strong-field,  $\alpha$ -diimine ligands such as those in the present study.<sup>31</sup> Spectra for the binuclear  $[\text{Fe}^{\text{II}}(\text{bipym})\text{Cu}^{\text{II}}]$  and  $[\text{Fe}^{\text{II}}(\text{bipym})\text{Zn}^{\text{II}}]$  complexes, shown in Figures 3c and 3d, appear very similar with both species having intense absorption bands in the 550- and 750-nm regions. However, the relative intensities of the bands differ substantially for the two complexes, with those for the  $\text{Cu}^{\text{II}}$  derivative being approximately twice as intense as for the  $\text{Zn}^{\text{II}}$  complex. Finally, Figure 4 displays the comparative absorption spectra in the visible for  $[\text{Cu}^{\text{II}}(\text{acac})_2]$ ,  $[\text{Fe}^{\text{II}}(\text{C}_{18}\text{H}_{18}\text{N}_6)(\text{bipym})]^{2+}$ , and  $[\text{Fe}^{\text{II}}(\text{C}_{18}\text{H}_{18}\text{N}_6)(\text{bipym})\text{Cu}^{\text{II}}(\text{acac})_2]^{2+}$  in  $\text{CH}_2\text{Cl}_2$ . These spectra serve to conclusively demonstrate that the  $[\text{Fe}^{\text{II}}(\text{bipym})\text{Cu}^{\text{II}}]$  complex is, indeed, a discrete species in solution in that its spectrum is not simply an addition spectrum of the  $[\text{Fe}^{\text{II}}(\text{C}_{18}\text{H}_{18}\text{N}_6)(\text{bipym})]^{2+}$  and  $[\text{Cu}^{\text{II}}(\text{acac})_2]$  components.

Solution conductivities of B, C, and D obtained in  $\text{CH}_2\text{Cl}_2$  indicate strong ion pairing in solution, with the values being  $\leq 7$  mho  $\text{M}^{-1} \text{cm}^{-1}$ . The instability of the binuclear complexes in coordinating solvents such as  $\text{CH}_3\text{CN}$ ,  $\text{MeOH}$ , or  $\text{Me}_2\text{SO}$  is likely due, in part, to the iron(II) spin state. The monomeric  $[\text{Fe}^{\text{II}}(\text{C}_{18}\text{H}_{18}\text{N}_6)(\text{bipym})]^{2+}$  cation possesses a magnetic moment of  $1.60 \mu_{\text{B}}$  in  $\text{CH}_2\text{Cl}_2$  at 298 K. This value, although somewhat higher than normal for low-spin  $\text{Fe}^{\text{II}}$ , is indicative of an essentially low-spin center. Solid-state magnetic and Mössbauer data, given below, also support a low-spin assignment for  $[\text{Fe}^{\text{II}}(\text{C}_{18}\text{H}_{18}\text{N}_6)(\text{bipym})](\text{ClO}_4)_2$ . However, the  $[\text{Fe}^{\text{II}}(\text{C}_{18}\text{H}_{18}\text{N}_6)(\text{bipym})\text{M}^{\text{II}}(\text{acac})_2]^{2+}$  cations are both high spin in solution with magnetic moments of  $5.89$  ( $\text{M} = \text{Cu}^{\text{II}}$ ) and  $4.80 \mu_{\text{B}}$  ( $\text{M} = \text{Zn}^{\text{II}}$ ) in  $\text{CH}_2\text{Cl}_2$  at 298 K. Hence, the high-spin binuclear complexes do not benefit from the added CFSE of a low-spin center, which could be a contributory factor leading to dissociation into low-spin mononuclear species. Finally, the binuclear complexes also probably suffer some instability (relative to the low-spin bis- $\text{CH}_3\text{CN}$  complex) due to "strain energy" required in folding their macrocyclic unit, as well as due to the rather close placement (6-7 Å) of two positively charged metal centers separated by only a neutral bipym bridge. Studies in progress employing negatively charged 2-(pyrimidyl)imidazolate and 2,2'-biimidazolate bridges suggest the latter factor to be of considerable importance.<sup>32</sup>

The difference in the  $\text{Fe}^{\text{II}}$  spin state between the mononuclear and binuclear complexes is also reflected in the  $\text{Fe}^{\text{II}} \rightleftharpoons \text{Fe}^{\text{III}}$  redox behavior, as determined electrochemically. Cyclic

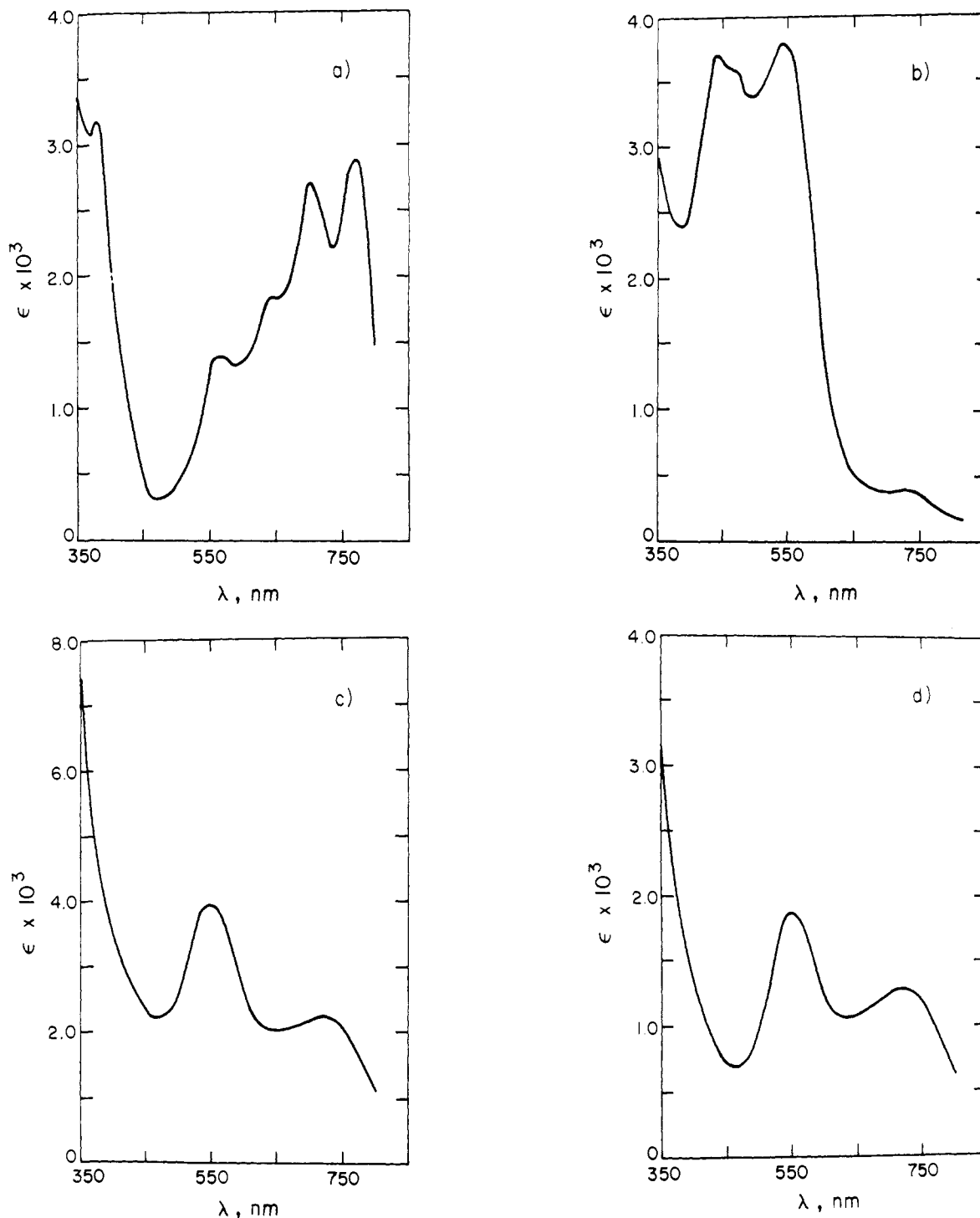


**Figure 3.** Room temperature electronic absorption spectrum of (a)  $[\text{Fe}^{\text{II}}(\text{C}_{18}\text{H}_{18}\text{N}_6)(\text{CH}_3\text{CN})_2](\text{ClO}_4)_2$  in  $\text{CH}_3\text{CN}$ ; (b)  $[\text{Fe}^{\text{II}}(\text{C}_{18}\text{H}_{18}\text{N}_6)(\text{bipym})](\text{ClO}_4)_2$  in  $\text{CH}_2\text{Cl}_2$ ; (c)  $[\text{Fe}^{\text{II}}(\text{C}_{18}\text{H}_{18}\text{N}_6)(\text{bipym})\text{Cu}^{\text{II}}(\text{acac})_2](\text{ClO}_4)_2$  in  $\text{CH}_2\text{Cl}_2$ ; (d)  $[\text{Fe}^{\text{II}}(\text{C}_{18}\text{H}_{18}\text{N}_6)(\text{bipym})\text{Zn}^{\text{II}}(\text{acac})_2](\text{ClO}_4)_2$  in  $\text{CH}_2\text{Cl}_2$ .

voltammograms for the three complexes are shown in Figure 5. As seen in the figure, the low-spin  $[\text{Fe}^{\text{II}}(\text{C}_{18}\text{H}_{18}\text{N}_6)(\text{bipym})]^{2+}$  complex has  $E_{1/2}$  of ca. +1.30 V (SCE) for the  $\text{Fe}^{\text{II}}/\text{Fe}^{\text{III}}$  couple in  $\text{CH}_2\text{Cl}_2$ . At scan rates of  $\leq 0.10$  V/s, the reduced  $[\text{Fe}^{\text{II}}(\text{C}_{18}\text{H}_{18}\text{N}_6)(\text{bipym})]^{2+}$  complex did not yield a cathodic wave (Figure 5a). However, the anodic peak current is proportional to  $V^{1/2}$  at high scan rates and  $|E_p - E_{p/2}| = 60 \pm 10$  mV, suggesting a reversible, one-electron transfer followed by a rapid chemical reaction (EC mechanism).<sup>33</sup> Reversible peaks were obtained at scan rates  $> 1.0$  V/s. Cyclic voltammograms for the high-spin binuclear complexes (Figures 5b and 5c) show a large 700-mV decrease in  $E_{1/2}$  for the  $\text{Fe}^{\text{II}}/\text{Fe}^{\text{III}}$  couple and give an identical value of +0.60 V

( $\pm 0.01$  V by differential pulse polarography) for both the  $\text{Cu}^{\text{II}}$  and  $\text{Zn}^{\text{II}}$  derivatives. Both cyclic voltammograms also appear reversible at scan rates of  $> 0.10$  V/s, with no indication of compound decomposition. These electrochemical results are of particular significance since they (1) further establish that the  $[\text{Fe}^{\text{II}}(\text{bipym})\text{M}^{\text{II}}]$  compounds are, indeed, discrete entities in solution with  $\text{Fe}^{\text{II}} \rightleftharpoons \text{Fe}^{\text{III}}$  redox behavior differing from the mononuclear precursor, and (2) serve to suggest that the paramagnetic  $\text{Cu}^{\text{II}}$  center in C has little, if any, electronic interaction (i.e., magnetic exchange) with its  $\text{Fe}^{\text{II}}$  partner across the bipym bridge. It is tempting to attribute the difference in  $E_{1/2}$  between the low-spin compound (B) and its high-spin binuclear relatives (C and D) to the difference in the  $\text{Fe}^{\text{II}}$  spin

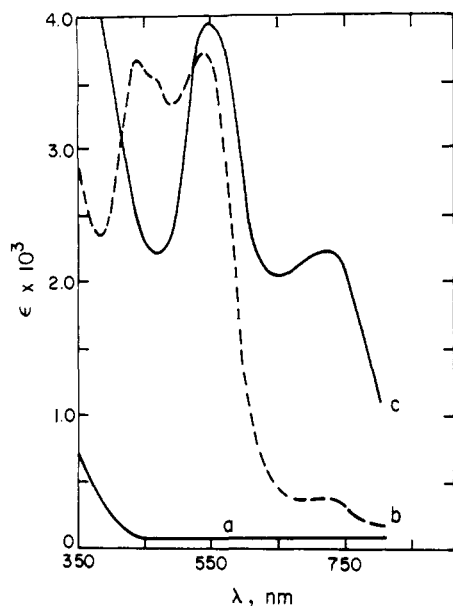


**Figure 4.** Comparative electronic absorption spectra in  $\text{CH}_2\text{Cl}_2$  for (a)  $[\text{Cu}^{\text{II}}(\text{acac})_2]$ ; (b)  $[\text{Fe}^{\text{II}}(\text{C}_{18}\text{H}_{18}\text{N}_6)(\text{bipym})](\text{ClO}_4)_2$ ; (c)  $[\text{Fe}^{\text{II}}(\text{C}_{18}\text{H}_{18}\text{N}_6)(\text{bipym})\text{Cu}^{\text{II}}(\text{acac})_2](\text{ClO}_4)_2$ .

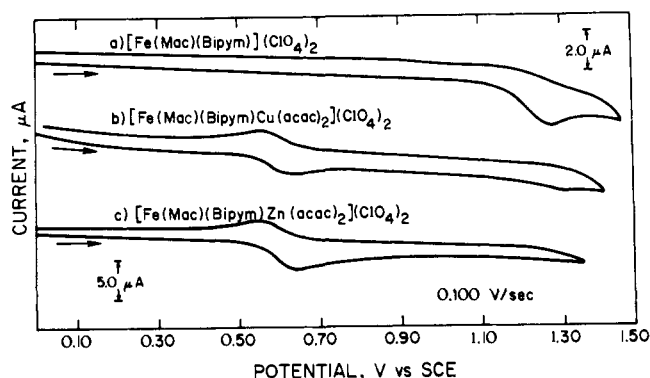


**Figure 5.** Cyclic voltammograms of the  $\text{Fe}^{\text{II}}/\text{Fe}^{\text{III}}$  couple for the complexes obtained in  $\text{CH}_2\text{Cl}_2$  at platinum button electrodes. Positions are referenced relative to SCE. (Mac =  $\text{C}_{18}\text{H}_{18}\text{N}_6$  in the text.)

state; however, available electrochemical data on the variable-spin  $[\text{Fe}^{\text{II}}(\text{x-py})_3\text{tren}]^{2+}$  and  $[\text{Fe}^{\text{III}}(\text{dtc})_3]$  systems,<sup>34,35</sup> as well as more recent variable-temperature data on the  $[\text{Fe}^{\text{III}}(\text{x-sal})_2\text{trien}]^+$  system,<sup>36,37</sup> indicate that the spin-state dependency of  $E_{1/2}$  will, in general, not exceed 100 mV. This being the case, the 700-mV difference between B and C or D arises mainly from a large substituent effect of the coordinated  $[\text{M}^{\text{II}}(\text{acac})_2]$  moiety. In fact, this same electronic substituent effect is apparently large enough to induce the low-spin  $\rightarrow$  high-spin conversion upon formation of the binuclear complexes, since molecular models suggest that the spin conversion is not of steric origin.<sup>24,38</sup> This interpretation is under investigation by structural work presently in progress on B, C, and D.<sup>39</sup> Assuming the  $[\text{Cyt } a_3(\text{imid})\text{Cu}_U]$  model of Figure 1 to be correct for oxidase, a similar substituent effect due to  $\text{Cu}_U$  might account for the fact that Cyt  $a_3$  is thought to always be high spin in all of its naturally occurring redox chemistry.<sup>40</sup> Finally, an attempt has been made to identify a  $\text{Cu}^{\text{II}}/\text{Cu}^{\text{I}}$  redox couple for C (Figure 6). Comparison of Figures 6a and 6b indicates that the wave at  $-0.24$  V may be due to the  $\text{Cu}^{\text{II}} \rightarrow \text{Cu}^{\text{I}}$  reduction process. The other reduction waves at ca.  $-0.77$ ,  $-1.05$ , and  $-1.40$  V are most likely ligand-centered reductions.

**Magnetic Susceptibility Data.** The  $[\text{Fe}^{\text{II}}(\text{C}_{18}\text{H}_{18}\text{N}_6)(\text{bipym})](\text{ClO}_4)_2$  compound has a magnetic moment of 1.52

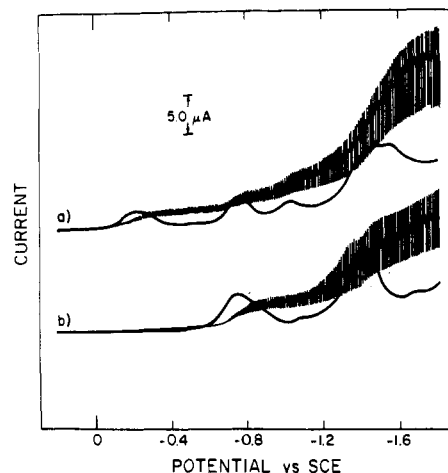


**Figure 6.** Polarograms and differential pulse polarograms at DME in  $\text{CH}_2\text{Cl}_2$  for (a)  $[\text{Fe}^{\text{II}}(\text{C}_{18}\text{H}_{18}\text{N}_6)(\text{bipym})\text{Cu}^{\text{II}}(\text{acac})_2](\text{ClO}_4)_2$ ; (b)  $[\text{Fe}^{\text{II}}(\text{C}_{18}\text{H}_{18}\text{N}_6)(\text{bipym})\text{Zn}^{\text{II}}(\text{acac})_2](\text{ClO}_4)_2$ . Polarography conditions: scan rate = 10 mV/s, drop time = 0.5 s. Differential pulse polarography conditions: scan rate = 10 mV/s, pulse time = 0.5 s, modulation amplitude = 25 mV.

$\mu_B$  at 298 K, which gradually decreases to  $1.30 \mu_B$  by 83 K. While this value is somewhat above that expected for low-spin  $\text{Fe}^{\text{II}}$ , nevertheless, it is in good agreement with the solution moment and indicative of an essentially low-spin center. Upon chelation with  $\text{M}(\text{acac})_2$  to form the  $[\text{Fe}^{\text{II}}(\text{C}_{18}\text{H}_{18}\text{N}_6)(\text{bipym})\text{M}^{\text{II}}(\text{acac})_2](\text{ClO}_4)_2$  binuclear species, the  $\text{Fe}^{\text{II}}$  center converts to fully high spin with  $\mu_{\text{eff}}(304 \text{ K}) = 5.46$  ( $\text{Cu}^{\text{II}}$ ) and  $\mu_{\text{eff}}(299 \text{ K}) = 5.11$  ( $\text{Zn}^{\text{II}}$ ). A value of  $5.11 \mu_B$  for the  $[\text{Fe}^{\text{II}}(\text{bipym})\text{Zn}^{\text{II}}]$  case is that expected for an  $S = 2$  iron center with an appreciable orbital contribution. Assuming the same  $\mu_{\text{eff}}$  value for  $\text{Fe}^{\text{II}}$  in  $[\text{Fe}^{\text{II}}(\text{bipym})\text{Cu}^{\text{II}}]$ , the  $\text{Cu}^{\text{II}}$  center contributes  $\sim 1.9 \mu_B$  to the total observed magnetic moment of  $5.46 \mu_B$ . This is a common value for magnetically dilute  $\text{Cu}^{\text{II}}$ , indicating that the room temperature electronic ground state for the complex is best viewed as *isolated*  $S = 2$  and  $S = 1/2$  spins. Strong antiferromagnetic  $[\text{Fe}^{\text{II}}-\text{Cu}^{\text{II}}]$  coupling of the magnitude present in resting oxidase ( $-J \geq 200 \text{ cm}^{-1}$ ) would, of course, yield a net  $S = 3/2$  state while a strong ferromagnetic interaction would result in an overall  $S = 5/2$  state.

Variable-temperature susceptibility data from 8 to 300 K for the binuclear complexes are displayed in Figure 7 and tabulated in Table II (microfilm). The  $[\text{Fe}^{\text{II}}(\text{bipym})\text{Cu}^{\text{II}}]$  compound shows a gradual decrease in magnetic moment from  $5.46$  to  $5.15 \mu_B$  by 83 K, but below 80 K the moment decreases rapidly to  $4.05 \mu_B$  by 8.3 K. This behavior could be attributed to a moderate antiferromagnetic exchange interaction across the bipym bridge were it not for the fact that the  $[\text{Fe}^{\text{II}}(\text{bipym})\text{Zn}^{\text{II}}]$  center exhibits a very similar  $\mu_{\text{eff}}$  vs. temperature pattern where exchange is impossible. In fact, at each temperature, the observed difference in  $\mu_{\text{eff}}$  between the  $\text{Cu}^{\text{II}}$  and  $\text{Zn}^{\text{II}}$  derivatives corresponds almost exactly to that expected due to the additional paramagnetism of an isolated  $S = 1/2$  spin. In view of this behavior, the non-Curie behavior at low temperatures for both  $[\text{Fe}^{\text{II}}(\text{C}_{18}\text{H}_{18}\text{N}_6)(\text{bipym})\text{M}^{\text{II}}(\text{acac})_2](\text{ClO}_4)_2$  compounds is probably of the same origin, with an  $\text{Fe}^{\text{II}}$  (high-spin)  $\rightleftharpoons$  (low-spin) spin equilibrium and/or zero-field splitting of the  $S = 2$  iron center being likely candidates. While the former explanation is a possibility, especially since the  $[\text{Fe}^{\text{II}}(\text{C}_{18}\text{H}_{18}\text{N}_6)(\text{bipym})]^{2+}$  precursor is low spin, spin-equilibrium systems are relatively rare<sup>41</sup> and available Mössbauer data (vide infra) are inconsistent with this interpretation. Therefore, it appears that zero-field splitting of the isolated  $S = 2$  iron center is the most likely explanation for the observed variable-temperature magnetic behavior. In fact, the data between 10 and 40 K closely resembles that for high-spin

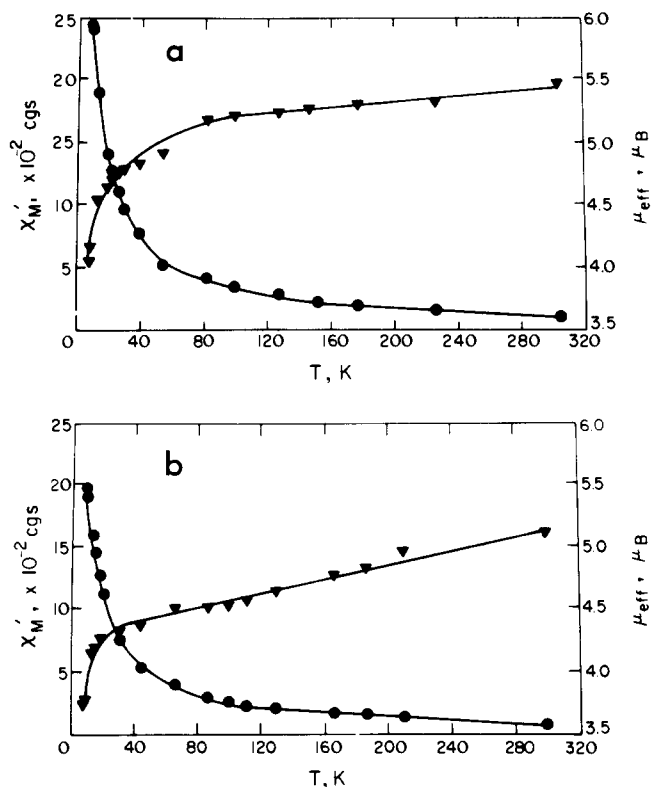


**Figure 7.** (a)  $\mu_{\text{eff}}$  vs. temperature ( $\blacktriangledown$ ) and  $\chi_{M'}$  vs. temperature ( $\bullet$ ) plots for  $[\text{Fe}^{\text{II}}(\text{C}_{18}\text{H}_{18}\text{N}_6)(\text{bipym})\text{Cu}^{\text{II}}(\text{acac})_2](\text{ClO}_4)_2$ . (b)  $\mu_{\text{eff}}$  vs. temperature ( $\blacktriangledown$ ) and  $\chi_{M'}$  vs. temperature ( $\bullet$ ) plots for  $[\text{Fe}^{\text{II}}(\text{C}_{18}\text{H}_{18}\text{N}_6)(\text{bipym})\text{Zn}^{\text{II}}(\text{acac})_2](\text{ClO}_4)_2$ .

**Table III.** Mössbauer Spectral Parameters for the Monomeric and  $\mu$ -Bipyrimidyl Iron(II) Compounds

compd	$\delta$ , mm $s^{-1}$ <i>a, b</i>	$\Delta E_Q$ , mm $s^{-1}$ <i>b</i>
$[\text{Fe}^{\text{II}}(\text{C}_{18}\text{H}_{18}\text{N}_6)(\text{CH}_3\text{CN})_2](\text{ClO}_4)_2$	0.52 (0.01)	1.66 (0.02)
$[\text{Fe}^{\text{II}}(\text{C}_{18}\text{H}_{18}\text{N}_6)(\text{bipym})](\text{ClO}_4)_2$	0.60 (0.02)	0.66 (0.03)
$[\text{Fe}^{\text{II}}(\text{C}_{18}\text{H}_{18}\text{N}_6)(\text{bipym})\text{Cu}^{\text{II}}(\text{acac})_2](\text{ClO}_4)_2$	1.27 (0.03)	1.87 (0.04)
$[\text{Fe}^{\text{II}}(\text{C}_{18}\text{H}_{18}\text{N}_6)(\text{bipym})\text{Zn}^{\text{II}}(\text{acac})_2](\text{ClO}_4)_2$	1.26 (0.02)	1.88 (0.03)

<sup>a</sup> Spectra were taken at 100 K and referenced relative to a room temperature sodium nitroprusside (SNP) spectrum. <sup>b</sup> Standard deviations in parentheses.

$\text{Fe}^{\text{II}}$  porphyrin complexes where  $D$  (the zero-field splitting parameter) is typically  $\geq 5 \text{ cm}^{-1}$ .<sup>42</sup>

**Mössbauer Data.** The  $^{57}\text{Fe}$  Mössbauer spectra of A, B, C, and D obtained at 100 K are shown in Figure 8 with the computer-fit isomer shift and quadrupole splitting parameters listed in Table III. Compound A contains low-spin  $\text{Fe}^{\text{II}}$  ( $\mu_{\text{eff}}(100 \text{ K}) = 0.6 \mu_{\text{B}}$ ) and displays an isomer shift of 0.52 which is typical of the spin state.<sup>43</sup> The large quadrupole splitting of  $1.66 \text{ mm s}^{-1}$  is somewhat unusual, but not necessarily so in view of the tetragonal distortion exhibited by the molecule ( $\text{Fe}-\text{N}_{(\text{Mac})} = 1.90 \text{ \AA}$ ;  $\text{Fe}-\text{NCCH}_3 = 1.94 \text{ \AA}$ ).<sup>27</sup> Compound B, also low spin, has a spectrum which is more typical of  $S = 0$  iron(II). Both of the  $\mu$ -bipyrimidyl compounds, C and D, contain high-spin  $\text{Fe}^{\text{II}}$  and possess large  $\delta$  and  $\Delta E_Q$  values which are characteristic of the  $S = 2$  spin state.<sup>43</sup> Furthermore, within experimental error, the  $[\text{Fe}^{\text{II}}(\text{bipym})\text{M}^{\text{II}}]$  compounds ( $\text{M} = \text{Cu}^{\text{II}}$  or  $\text{Zn}^{\text{II}}$ ) possess *identical* isomer shift and quadrupole splitting values. This result further collaborates the above electrochemical and magnetic susceptibility data in establishing essentially identical high-spin electronic envi-

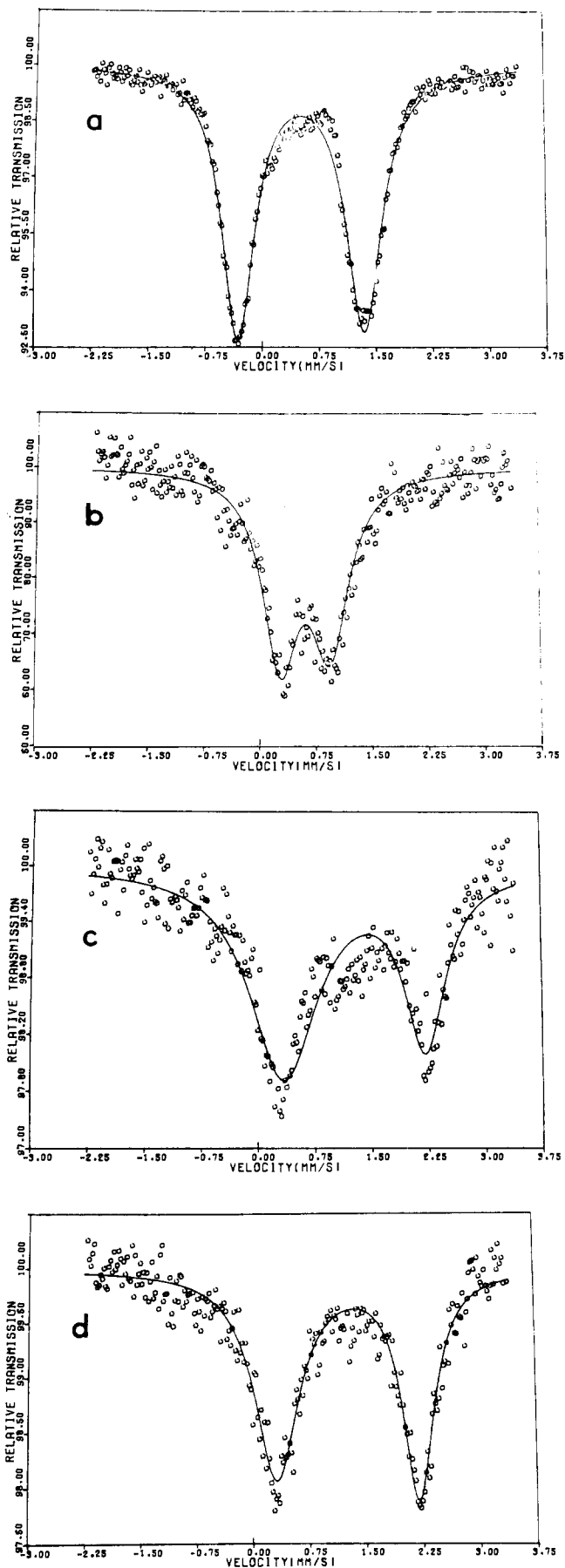


**Figure 8.**  $^{57}\text{Fe}$  Mössbauer spectrum at 100 K for (a)  $[\text{Fe}^{\text{II}}(\text{C}_{18}\text{H}_{18}\text{N}_6)(\text{CH}_3\text{CN})_2](\text{ClO}_4)_2$ ; (b)  $[\text{Fe}^{\text{II}}(\text{C}_{18}\text{H}_{18}\text{N}_6)(\text{bipym})](\text{ClO}_4)_2$ ; (c)  $[\text{Fe}^{\text{II}}(\text{C}_{18}\text{H}_{18}\text{N}_6)(\text{bipym})\text{Cu}^{\text{II}}(\text{acac})_2](\text{ClO}_4)_2$ ; (d)  $[\text{Fe}^{\text{II}}(\text{C}_{18}\text{H}_{18}\text{N}_6)(\text{bipym})\text{Zn}^{\text{II}}(\text{acac})_2](\text{ClO}_4)_2$ .

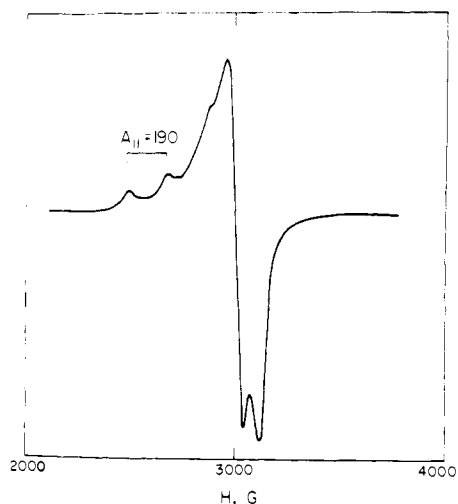


**Figure 9.** EPR spectrum of  $[\text{Fe}^{\text{II}}(\text{C}_{18}\text{H}_{18}\text{N}_6)(\text{bipym})\text{Cu}^{\text{II}}(\text{acac})_2](\text{ClO}_4)_2$  in a  $\text{CH}_2\text{Cl}_2$  glass at 8 K.

ronments for  $\text{Fe}^{\text{II}}$  within the two compounds, and thus noninteracting  $[\text{Fe}^{\text{II}}-\text{Cu}^{\text{II}}]$  centers in C. In particular, there is no evidence of a six-line magnetic hyperfine spectrum for the  $\text{Cu}^{\text{II}}$  derivative of the nature that might be present if  $[\text{Fe}^{\text{II}}-\text{Cu}^{\text{II}}]$  antiferromagnetic exchange were operative.<sup>44</sup>

The Mössbauer spectra for C and D also offer evidence for the absence of high-spin ( $S = 2$ )  $\rightleftharpoons$  low-spin ( $S = 0$ ) spin-equilibrium processes which could explain the observed temperature dependency of the magnetic susceptibility. In particular, for the  $[\text{Fe}^{\text{II}}(\text{bipym})\text{Zn}^{\text{II}}]$  compound,  $\mu_{\text{eff}}(100 \text{ K}) = 4.5 \mu_{\text{B}}$ . Assuming high- and low-spin limiting magnetic moments of 5.1 and  $0.5 \mu_{\text{B}}$ , respectively, for the two spin states, the low-spin isomer would be  $\sim 25\%$  populated for the observed  $4.5 \mu_{\text{B}}$  value. Furthermore, assuming that a Mössbauer spectrum similar to that of B would result for a supposed low-spin form of D, it seems likely that the observed spectrum for D would reflect some presence of the low-spin state,<sup>34,45,46</sup> especially by the presence of a peak centered at  $\sim 0.94 \text{ mm s}^{-1}$ . Thus, available information suggests that the observed non-Curie magnetic behavior at low temperature for C and D is not due to a spin-equilibrium process, but lower temperature Mössbauer data are needed to establish this beyond doubt.

**EPR Data.** The EPR spectrum of C in a  $\text{CH}_2\text{Cl}_2$  glass at 8 K is shown in Figure 9. The spectrum is typical of magnetically dilute  $S = 1/2$  copper(II), with copper nuclear hyperfine (190 G) seen only on the  $g_{\parallel}$  component. In particular, there are no other spectral features identifiable with an  $S = 3/2$  spin state which would be highly populated by 8 K ( $4.0 \mu_{\text{B}}$ ) if an  $[\text{Fe}^{\text{II}}-\text{Cu}^{\text{II}}]$  antiferromagnetic interaction were responsible for the anomalous low-temperature magnetic susceptibility data. Therefore, when interpreted together, the above susceptibility and Mossbauer data, and the present EPR results, all argue convincingly for noninteracting  $S = 2$  and  $S = 1/2$  spins in C, again leaving the low-temperature magnetic susceptibility behavior of both C and D best rationalized in terms of zero-field splitting of isolated  $S = 2$  iron(II) centers. These  $S = 2$  centers are, of course, expected to be EPR silent themselves owing to the relatively large magnitude of  $D$  ( $\gtrsim 5 \text{ cm}^{-1}$ ) usually found for high-spin iron(II).<sup>42</sup>

Finally, it is noted that integration of the EPR signal of Figure 9 accounts for  $\geq 90\%$  of the copper present in the sample. Thus, there is no appreciable loss of EPR intensity, or relaxation broadening, associated with the presence of the high-spin  $\text{Fe}^{\text{II}}$  center which is possibly capable of a dipolar interaction ( $^5\text{T}$  ground state) with the  $\text{Cu}^{\text{II}}$  ion only  $6\text{--}7 \text{ \AA}$  away.<sup>47</sup> Such a dipolar interaction between  $\text{Cyt } a^{3+}$  and  $\text{Cu}_D^{2+}$  in cytochrome oxidase has been proposed by Leigh<sup>48</sup> to be

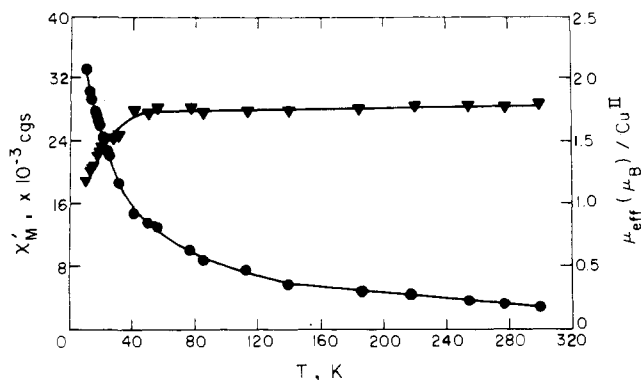


**Figure 10.**  $\mu_{\text{eff}}$  vs. temperature ( $\blacktriangledown$ ) and  $\chi_{\text{M}}'$  vs. temperature ( $\bullet$ ) plots for  $[(\text{hfac})_2\text{Cu}^{\text{II}}(\text{bipym})\text{Cu}^{\text{II}}(\text{hfac})_2]$ . The solid line is a least-squares fit to the Bleaney-Bowers equation.

responsible for the loss of EPR intensity (without signal broadening or line-shape change)<sup>49</sup> of the  $\text{Cu}_D^{2+}$  signal such that the center appears only 80% EPR active. However, as has been recently pointed out by Palmer,<sup>50</sup> in the case of metalloproteins where EPR resonances are intrinsically broad, due to anisotropy in  $g$ , any dipolar field would have to be large with respect to the intrinsic line width if a significant loss in intensity due to the Leigh effect is to be expected. This requirement has frequently led to ridiculously small values of  $r$  (the magnitude of the dipolar field is proportional to  $r^{-3}$ ) for which other effects such as magnetic exchange would almost certainly dominate. The Leigh effect is, therefore, not likely to be as influential for metalloproteins as for simple model compounds with narrower line widths; however, it does not seem to be important for the present  $[\text{Fe}^{\text{II}}(\text{bipym})\text{Cu}^{\text{II}}]$  complex where the  $[\text{Fe}-\text{Cu}]$  separation is  $6\text{--}7 \text{ \AA}$ .<sup>47</sup> In contrast, the recently reported nonbridged  $[\text{Fe}^{\text{II}} \cdots \text{Cu}^{\text{II}}]$  tetrakis(pyridine) capped porphyrin compound of Buckingham et al. is apparently EPR silent for an  $[\text{Fe}-\text{Cu}]$  distance of  $\sim 6 \text{ \AA}$ .<sup>51</sup> Whether or not this is due to the Leigh effect or to dipolar relaxation broadening, in general, has yet to be established.

**A  $[\text{Cu}^{\text{II}}(\text{bipym})\text{Cu}^{\text{II}}]$  Center.** In order to examine a  $\mu$ -bipyrimidyl case other than the mixed-metal system, the  $\text{Cu}_2$  compound,  $[(\text{hfac})_2\text{Cu}^{\text{II}}(\text{bipym})\text{Cu}^{\text{II}}(\text{hfac})_2]$ , was prepared and characterized (see Experimental Section) to address three questions: (1) Is bipym capable of fostering magnetic exchange in a pure-metal system? (2) If so, how does the magnitude of the exchange compare to that for other known  $\text{Cu}_2$  systems with N-heterocyclic bridges, including imidazolate? Finally, (3) with answers to (1) and (2), what can be said about the  $[\text{Fe}^{\text{II}}(\text{bipym})\text{Cu}^{\text{II}}]$  results as they relate to the possible  $[\text{Fe}^{\text{III}}(\text{imid})\text{Cu}^{\text{II}}]$  active site structure of cytochrome oxidase?

Variable-temperature (10–300 K) magnetic susceptibility data obtained for  $[(\text{hfac})_2\text{Cu}^{\text{II}}(\text{bipym})\text{Cu}^{\text{II}}(\text{hfac})_2]$  are shown in Figure 10, with the actual data presented in Table IV (microfilm). As seen from the figure, the  $\chi_{\text{M}}'$  vs. temperature data are characteristic of an antiferromagnetic exchange interaction. The compound is, of course, an  $S_1 = S_2 = 1/2$  exchange interacting species and the variation in the molar susceptibility with temperature is represented by the Bleaney-Bowers equation<sup>52</sup>

$$\chi_{\text{M}} = \frac{N\bar{g}^2\beta^2}{kT} \left[ \frac{2}{3 + \exp(-2J/kT)} \right] + N\alpha \quad (1)$$

In the equation,  $N$  is Avogadro's number,  $\bar{g}$  is the average electronic  $g$  factor,  $\beta$  is the Bohr magneton,  $k$  is the Boltzmann constant,  $T$  is the temperature,  $-J$  is the parameter which gauges the magnitude of the antiferromagnetic exchange interaction, and  $N\alpha$  is the TIP correction. The data in Table IV

**Table V.** Magnetic Exchange Data for Some Pure- and Mixed-Metal Binuclear Centers with N-Heterocyclic Bridges

compd	bridge	M-M distance, Å	-J, cm <sup>-1</sup>	ref
[Cu <sup>II</sup> (pyz)(NO <sub>3</sub> ) <sub>2</sub> ] <sub>2</sub>	pyrazine	6.71	6	a
[Cu <sup>II</sup> (acac)(pz)] <sup>3+</sup>	pyrazolyl		35	b
[Cu <sup>II</sup> <sub>2</sub> (bpimid)] <sup>4+</sup>	imidazolate	6.21 (est)	81.3	15, 16
[Cu <sup>II</sup> <sub>2</sub> (bpimid)(imid)] <sub>2</sub>	imidazolate	6.21 (Cu <sub>1</sub> -Cu <sub>2</sub> )	87.4	15, 16
	imidazolate	5.91 (C7 <sub>1</sub> -Cu <sub>2</sub> )	30	
[Cu <sup>II</sup> (pip)] <sub>2</sub> (imid) <sup>3+</sup>	imidazolate	5.93 (est)	26.1	16
[Cu <sup>II</sup> <sub>2</sub> (Me <sub>3</sub> dien) <sub>2</sub> (biimid)](BPh <sub>4</sub> ) <sub>2</sub>	biimidazolate	5.49	<0.5	18a
[(byp) <sub>2</sub> ClRu <sup>III</sup> ] <sub>2</sub> (pyz)	pyrazine	6.9	~0	c
[(Cp <sub>2</sub> Ti <sup>III</sup> )] <sub>2</sub> (biimid)	biimidazolate	6.02	25.2	18b
[(Cp <sub>2</sub> Ti <sup>III</sup> )] <sub>2</sub> (bibimid)	bibenzimidazolate	6.02	19.5	18b
[Mn <sup>II</sup> (TPP)(imid)(THF)] <sub>n</sub>	imidazolate	6.54	<<8	14
[Fe <sup>III</sup> (TPP)(imid)(THF)] <sub>n</sub>	imidazolate	6.5 (est)	<2	14
Proteins				
superoxide dismutase (Cu <sup>II</sup> derivative)	imidazolate	6.0 (est)	26	13
superoxide dismutase (Co <sup>II</sup> derivative)	imidazolate	6.0 (est)	>300	19
cytochrome oxidase (fully oxidized)	imidazolate (?)		≥200	8
cytochrome oxidase (fully oxidized; CN <sup>-</sup> derivative)	imidazolate (?)		~40	8

<sup>a</sup> Juan F. Villa and W. E. Hatfield, *J. Am. Chem. Soc.*, **93**, 4081 (1971). <sup>b</sup> C. G. Barraclough, R. W. Brookes, and R. L. Martin, *Aust. J. Chem.*, **27**, 1843 (1974). <sup>c</sup> E. C. Johnson, R. W. Callahan, R. P. Eckbag, W. E. Hatfield, and T. J. Meyer, *Inorg. Chem.*, **18**, 618 (1979).

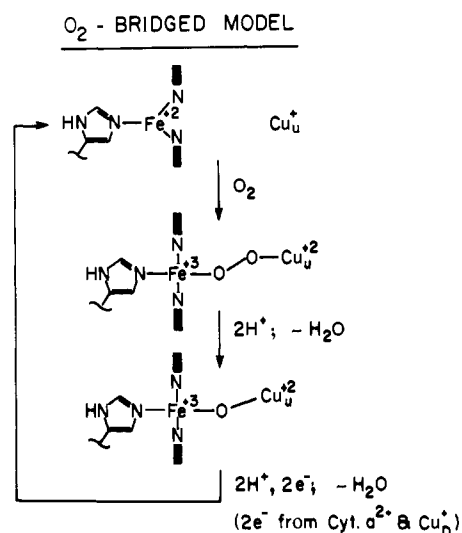


**Figure 11.** An alternative O<sub>2</sub>-bridged structural and catalytic redox model for the active site of cytochrome oxidase.

(microfilm) were least squares fit to eq 1, with  $N\alpha = 120 \times 10^{-6}$  cgs/mol of dimer, to yield  $\bar{g} = 2.12$  and  $-J = 7.9 \pm 1.0$  cm<sup>-1</sup>. This best fit to the susceptibility data is illustrated by the solid lines in Figure 10.

Table V presents a collection of  $-J$  values for several synthetic binuclear compounds, many of which contain imidazolate or related bridges with known M-M' distances. For these systems,  $-J$  ranges from ~0 to 90 cm<sup>-1</sup> and the present [(hfac)<sub>2</sub>Cu<sup>II</sup>(bipym)Cu<sup>II</sup>(hfac)<sub>2</sub>] compound ( $-J = 7.9$  cm<sup>-1</sup>) clearly falls within the lower end of this range. While the exact value of  $-J$  is undoubtedly a complicated function of the orbital energies and the geometrical arrangement of the bridge and metal orbitals participating in the exchange interaction, the present [Cu<sup>II</sup>(bipym)Cu<sup>II</sup>] results, and most of the data in Table V, imply that heterocyclic bridges such as imid<sup>-</sup>, biimid<sup>2-</sup>, pyz, and bipym can foster antiferromagnetic exchange interactions, but only with  $-J \lesssim 100$  cm<sup>-1</sup>. For the examples in Table V, the only exception appears to be a mixed-metal cobalt(II) SOD derivative where  $-J \gtrsim 300$  cm<sup>-1</sup> has been reported for the [Cu<sup>II</sup>(imid)Co<sup>II</sup>] pair; this is a significant result as it relates to cytochrome oxidase (vide infra) and as such it needs to be further substantiated since the work appears to be somewhat ambiguous.<sup>19</sup>

**An Alternative O<sub>2</sub>-Bridging Model.** Two pieces of magnetochemical evidence support an [Fe<sup>III</sup>(imid)Cu<sup>II</sup>] structure for the active site of cytochrome oxidase: (1) the [Cu<sup>II</sup>(imid)-Co<sup>II</sup>] SOD result where  $-J \gtrsim 300$  cm<sup>-1</sup> for this mixed-metal imidazolate-bridged species<sup>19</sup> is as large as that measured for the [Fe<sup>III</sup>-Cu<sup>II</sup>] exchange interaction in resting oxidase, and (2) the CN<sup>-</sup> derivative of oxidase has  $-J \approx 40$  cm<sup>-1</sup>,<sup>8</sup> or a value more in line with the other examples in Table V (cyt a<sub>3</sub><sup>3+</sup> is low spin in the CN<sup>-</sup> derivative and high spin in the resting parent enzyme). On the other hand, the present [Fe<sup>II</sup>(bipym)Cu<sup>II</sup>] model compound with  $J \approx 0$  is not at all supportive of the imidazolate-bridge structure originally proposed by Palmer et al.<sup>7</sup> Furthermore, we have preliminary magnetic and EPR results in hand<sup>53</sup> for an imidazolate-bridged [(TPP)Fe<sup>III</sup>(imid)Cu<sup>II</sup>(imidH)DAP]<sup>+</sup> cation (derived from [Fe<sup>III</sup>(TPP)Cl]<sup>+</sup> and [Cu<sup>II</sup>(imidH)<sub>2</sub>DAP]<sup>2+</sup>)<sup>54</sup> which also indicates  $-J$  to be small (<20 cm<sup>-1</sup>) for a case that is a much closer structural analogue of the proposed active site than is the present  $\mu$ -bipyrimidyl species.

In view of the above conflicting and, as yet, inconclusive evidence for an imidazolate-bridged structure in oxidase, it is important to note that an alternative O<sub>2</sub>-bridged model, as depicted in Figure 11, also possesses considerable merit. This model, as proposed here as a possibility, is not new, but the inorganic precedent in support of such a model has not been fully appreciated until recently.<sup>58</sup> Like the imidazolate-bridged model, this O<sub>2</sub>-bridging alternative also seems to satisfy all the magnetic and spectroscopic data presently available for the protein,<sup>40</sup> including some preliminary EXAFS data<sup>56</sup> which indicated an [Fe<sup>II</sup>··Cu] separation of only ~3 Å in resting oxidase (~5 Å is needed for imid<sup>-</sup>). In the fully reduced enzyme in Figure 11, Cyt a<sub>3</sub><sup>2+</sup> is depicted as a five-coordinate, high-spin Fe<sup>II</sup> heme with an imidazole ligand located trans to the closely situated Cu<sup>II</sup> center with a cavity between the two metals. The parallels between this structure and the heme hydrophobic cavity structure of myoglobin or hemoglobin are both obvious and compelling. Insertion of O<sub>2</sub> between the two metals can then be viewed as producing, via oxidative addition, a transient  $\mu$ -dioxygen species which further reacts with 2H<sup>+</sup> to produce H<sub>2</sub>O and a stable mixed-metal  $\mu$ -oxo center. This isolable [Fe<sup>III</sup>-O-Cu<sup>II</sup>] form would then be postulated to be the fully oxidized resting form of the enzyme which requires that Cyt a<sub>3</sub><sup>3+</sup> be high spin and  $-J \gtrsim 200$  cm<sup>-1</sup> for the [Fe<sup>III</sup>-Cu<sup>II</sup>] exchange interaction through the oxo (or perhaps hydroxo) bridge. In fact, exchange interactions approaching



this magnitude are known to be commonplace for synthetic  $[\text{Fe}^{\text{III}}\text{-O-Fe}^{\text{III}}]$  centers, such as in  $[(\text{TPP})\text{Fe}]_2\text{O}$  where  $-J$  is  $\sim 150\text{ cm}^{-1}$ .<sup>59</sup> Furthermore, transient  $(\text{FeOOFe})^*$  species, reminiscent of the proposed  $(\text{FeOOCu})^*$  structure for oxidase, are undoubtedly intermediates in the formation of the thermodynamically more stable  $[\text{Fe}^{\text{III}}\text{-O-Fe}^{\text{III}}]$  compounds; in fact, one such  $(\text{FeOOFe})^*$  species has purportedly been detected at low temperatures.<sup>60</sup> Furthermore, oxyhemerythrin,<sup>61</sup> oxyhemocyanin,<sup>62</sup> and a recently reported oxyhemocyanin model compound<sup>54</sup> are also all likely to contain  $\mu$ -dioxygen centers like that proposed here for the oxidase intermediate. Unfortunately, it is not yet known whether  $\text{H}_2\text{O}$  is a product of the  $(\text{FeOOFe})^* \rightarrow [\text{Fe}^{\text{III}}\text{-O-Fe}^{\text{III}}]$  oxygen atom extrusion reaction, but in protic media it seems highly likely; by analogy, a similar  $(\text{FeOOCu})^* \rightarrow [\text{Fe}^{\text{III}}\text{-O-Cu}^{\text{II}}]$  extrusion scheme could also produce the required  $\text{H}_2\text{O}$  molecule for oxidase. While Figure 11 shows the imidazole to remain coordinated to iron in the  $[\text{Fe}^{\text{III}}\text{-O-Cu}^{\text{II}}]$  form, such may not be the case since hematsins like  $[(\text{TPP})\text{Fe}]_2\text{O}$  do not strongly react with additional axial ligands, except by cleavage of the  $[\text{Fe}^{\text{III}}\text{-O-Fe}^{\text{III}}]$  bridge. Upon formation of the  $\text{CN}^-$  derivative,  $\text{Cyt } a_3^{3+}$  converts to low spin and our susceptibility measurements have shown that  $-J$  drops to  $\sim 40\text{ cm}^{-1}$  as a function of this change in spin state.<sup>8,40</sup> In the  $\text{O}_2$ -bridged model, an attractive structure for this low-spin  $\text{CN}^-$  derivative would be  $[(\text{NC})\text{-Fe}^{\text{III}}\text{-O-Cu}^{\text{II}}]$  with a  $\text{CN}^-$  ligand substituted for the weaker field imidazole; or alternatively,  $\text{CN}^-$  may actually cleave and replace the oxo bridge, i.e.,  $[\text{Fe}^{\text{III}}\text{-(CN)-Cu}^{\text{II}}]$ . Finally, the catalytic redox cycle for the  $\text{O}_2$ -bridging model would be completed by a concomitant  $2e^-$  reduction of the  $[\text{Fe}^{\text{III}}\text{-O-Cu}^{\text{II}}]$  unit ( $2e^-$ 's from reduced  $\text{Cyt } a_3^{2+}$  and  $\text{Cu}_D^+$ ) and a second oxygen atom extrusion-protonation reaction to again generate a  $\text{H}_2\text{O}$  molecule and conclude the observed overall  $4e^-$  reduction of  $\text{O}_2$ :  $\text{O}_2 + 4\text{H}^+ + 4e^- \rightarrow 2\text{H}_2\text{O}$ . This final step in the proposed mechanism is supported by the fact that the  $2e^-$  electrochemical reduction of  $[(\text{TPP})\text{Fe}]_2\text{O}$  has been shown to result in reductive cleavage of the oxo bridge with the production of  $[(\text{TPP})\text{Fe}^{\text{II}}]$  and  $[(\text{TPP})\text{Fe}^{\text{II}}\text{OH}]^-$ .<sup>63</sup>

Clearly, a modeling approach which places redox-active iron and copper centers in close proximity continues as a strong synthetic challenge, but one that promises major rewards in elucidating mechanistic details of the catalytically important  $\text{O}_2 \rightarrow \text{H}_2\text{O}$  reaction of cytochrome oxidase.

**Acknowledgment.** We gratefully acknowledge The Robert A. Welch Foundation [Grants C-627 (L.J.W.) and E-680 (K.M.K.)], the National Science Foundation (CHE77-14594, L.J.W.), the National Institutes of Health (GM25172-02, K.M.K.), and the donors of the Petroleum Research Fund, administered by the American Chemical Society (L.J.W.), for support of this work. We also thank Mr. Ken Goldsby for preparing some of the 2,2'-bipyrimidine. In addition, we especially acknowledge and appreciate the many rewarding discussions held with Professor Graham Palmer about cytochrome oxidase. Finally, we thank Professor Christopher Reed for a preprint of ref 58, which was supplied while this manuscript was under review.

**Supplementary Material Available:** Variable-temperature magnetic susceptibility data for  $[\text{Fe}^{\text{II}}(\text{C}_{18}\text{H}_{18}\text{N}_6)(\text{bipym})\text{Cu}^{\text{II}}(\text{acac})_2](\text{ClO}_4)_2$  (Table II) and  $[(\text{hfac})_2\text{Cu}^{\text{II}}(\text{bipym})\text{Cu}^{\text{II}}(\text{hfac})_2]$  (Table IV) (3 pages). Ordering information is given on any current masthead page.

## References and Notes

- Abstracted in part from the Ph.D. Dissertation of R. H. Petty, William Marsh Rice University, 1979; also presented in part at the 174th National Meeting of the American Chemical Society, Anaheim, Calif., April 1978, Abstracts, No. INOR-178. Part 1 of this series: R. H. Petty and L. J. Wilson, *J. Chem. Soc., Chem. Commun.*, 483 (1978).
- (a) William Marsh Rice University; (b) University of Houston.
- Author to whom correspondence should be addressed.
- See, for example, A. L. Lehninger, "The Mitochondrion", W. A. Benjamin, New York, 1965.
- E. E. Griffiths and D. C. Wharton, *J. Biol. Chem.*, **236**, 1850 (1961).
- D. C. Wharton in "Inorganic Biochemistry", Vol. 2, G. L. Eichorn, Ed., American Elsevier, New York, 1973, p 960.
- G. T. Babcock, L. E. Vickery, and G. Palmer, *J. Biol. Chem.*, **251**, 7907 (1976).
- M. F. Tweedle, L. J. Wilson, L. Garcia-Iniguez, G. T. Babcock, and G. Palmer, *J. Biol. Chem.*, **252**, 8065 (1978). [Apparently, the presence of  $\text{Cyt } a_3^{3+}\text{-Cu}^{\text{II}2+}$  magnetic coupling was originally suggested by Van Gelder and Beinert (ref 10) and later treated theoretically by Griffith: J. S. Griffith, *Mol. Phys.*, **21**, 141 (1971)].
- G. Palmer, G. T. Babcock, and L. E. Vickery, *Proc. Natl. Acad. Sci. U.S.A.*, **73**, 2006 (1973).
- B. F. Van Gelder and H. Beinert, *Biochim. Biophys. Acta*, **189**, 1 (1969).
- M. F. J. Blokzijl-Homan and B. F. van Gelder, *Biochim. Biophys. Acta*, **234**, 493 (1971).
- J. S. Richardson, K. A. Thomas, B. H. Rubin, and D. C. Richardson, *Proc. Natl. Acad. Sci. U.S.A.*, **72**, 1349 (1975).
- J. A. Fee and R. G. Briggs, *Biochim. Biophys. Acta*, **400**, 439 (1975).
- J. T. Landrum, C. A. Reed, K. Hatano, and W. R. Scheidt, *J. Am. Chem. Soc.*, **100**, 3232 (1978).
- G. Kolks, C. R. Frihart, H. N. Rabinowitz, and S. J. Lippard, *J. Am. Chem. Soc.*, **98**, 5720 (1976).
- G. Kolks and S. J. Lippard, *J. Am. Chem. Soc.*, **99**, 5804 (1977).
- M. S. Haddad and D. N. Hendrickson, *Inorg. Chem.*, **17**, 2622 (1978).
- (a) M. S. Haddad, E. N. Duesler, and D. N. Hendrickson, *Inorg. Chem.*, **18**, 141 (1979); (b) B. F. Fieselmann, D. N. Hendrickson, and G. Stucky, *ibid.*, in press.
- A. Desideri, M. Cerdonio, F. Mogno, S. Vitale, L. Calabrese, D. Cocco, and G. Rotilio, *FEBS Lett.*, **89**, 83 (1978).
- (a) The claim of an in situ preparation of an  $[\text{Fe}^{\text{III}}(\text{TPP})(2\text{-meimid})\text{Cu}^{\text{II}}(\text{acac})_2]$  compound appeared while this manuscript was under review; however, the compound was not successfully isolated. T. Proserpi and A. A. G. Tomlinsong, *J. Chem. Soc., Chem. Commun.*, 196 (1979). (b) See, for example, D. A. Buckingham, M. J. Gunter, and L. N. Mander, *J. Am. Chem. Soc.*, **100**, 2899 (1978); D. A. Krost and G. L. McPherson, *ibid.*, **100**, 987 (1978); C. J. O'Connor, D. P. Freyberg, and E. Sinn, *Inorg. Chem.*, **18**, 1077 (1979), and references cited therein; Beale et al., *Inorg. Chim. Acta*, **33**, 113 (1979); O. Kahn, P. Tola, J. Galy, and H. Coudanne, *J. Am. Chem. Soc.*, **100**, 3931 (1978). (c) S. Kokot, C. M. Harris, and E. Sinn, *Aust. J. Chem.*, **25**, 45 (1972).
- R. H. Petty and L. J. Wilson, *J. Chem. Soc., Chem. Commun.*, 483 (1978) (part 1 of this series).
- M. F. Tweedle and L. J. Wilson, *Rev. Sci. Instrum.*, **49**, 1001 (1978).
- D. F. Evans, *J. Chem. Soc.*, 2003 (1959).
- B. L. Chrisman and T. A. Tumolillo, *Comput. Phys. Commun.*, **2**, 322 (1975).
- D. D. Bly and M. G. Mellon, *J. Org. Chem.*, **27**, 2945 (1962).
- P. Westcott, Ph.D. Dissertation, Colorado State University, 1971.
- V. L. Goedkin, Y. Park, S. M. Peng, and J. M. Morris, *J. Am. Chem. Soc.*, **96**, 7693 (1974).
- U. T. Mueller-Westerhoff, *Adv. Chem. Ser.*, **150**, 41 (1976).
- M. Hunziker and A. Ludi, *J. Am. Chem. Soc.*, **99**, 7370 (1977).
- E. V. Dose and L. J. Wilson, *Inorg. Chem.*, **17**, 2660 (1978).
- L. J. Wilson, D. Georges, and M. A. Hoselton, *Inorg. Chem.*, **14**, 2968 (1975).
- B. R. Welch and L. J. Wilson, unpublished results.
- R. S. Nicholson and I. Shain, *Anal. Chem.*, **36**, 706 (1964).
- M. Hoselton, L. J. Wilson, and R. S. Drago, *J. Am. Chem. Soc.*, **97**, 1722 (1975).
- R. Chant, A. R. Hendrickson, R. L. Martin, and N. M. Rhode, *Inorg. Chem.*, **14**, 1894 (1975).
- M. F. Tweedle and L. J. Wilson, *J. Am. Chem. Soc.*, **98**, 4824 (1976).
- K. M. Kadish, K. Das, D. Schaeper, C. L. Merrill, B. R. Welch, and L. J. Wilson, *J. Am. Chem. Soc.*, submitted for publication.
- See, for example, H. A. Goodwin and R. N. Sylva, *Aust. J. Chem.*, **21**, 83 (1968).
- E. Sinn and L. J. Wilson, to be published.
- G. Palmer, T. Antalis, G. T. Babcock, L. Garcia-Iniguez, M. F. Tweedle, L. J. Wilson, and L. E. Vickery, "Mechanisms of Oxidizing Enzymes", T. P. Singer and R. Ondarza, Eds., Elsevier North Holland Press, Amsterdam, 1978, p 222, and references cited therein.
- E. V. Dose, M. A. Hoselton, N. Sutin, M. F. Tweedle, and L. J. Wilson, *J. Am. Chem. Soc.*, **100**, 1141 (1978), and references cited therein.
- A. Tasaki, J. Otsuke, and M. Kotani, *Biochim. Biophys. Acta*, **140**, 284 (1967).
- See, for example, N. N. Greenwood and T. C. Gibb, "Mössbauer Spectroscopy", Chapman and Hall, London, 1971, p 91.
- W. Kundig, H. Bömmel, G. Constabaris, and R. H. Linquist, *Phys. Rev.*, **142**, 327 (1966).
- H. A. Goodwin and R. N. Sylva, *Aust. J. Chem.*, **21**, 83 (1968).
- D. M. L. Goodgame and A. A. S. C. Macado, *Inorg. Chem.*, **8**, 2031 (1969).
- Approximate distance based on Dreiding stereomodels.
- J. S. Leigh, Jr., *J. Chem. Phys.*, **52**, 2608 (1970).
- Unlike the results of classical spin-spin interaction where *signal broadening* occurs as a function of  $(r^{-3})(1 - 3 \cos^2 \theta)$  with  $r$  the distance between paramagnetic ions and  $\theta$  the angle between the field and the symmetry axis, the Leigh theory (ref 48) predicts only loss of *signal intensity* without appreciable broadening for the special case of large dipolar fields resulting from exceptionally small values of  $r$ . For exceptionally small  $r$ 's the magnitude of the dipolar field is substantial and an EPR spectrum will be observed for only those molecules for which the term  $(3 \cos^2 \theta - 1)$  is near zero ( $\theta \sim 54^\circ$ ). However, these molecules are only a small percentage of the total sample, and the remaining molecules experience a distribution of dipolar fields of magnitude sufficient to displace the EPR signal away

- from its unperturbed position and the signal is thus lost in the base line. As  $r$  is increased, the magnitude of the dipolar field ( $r^{-3}$ ) decreases and an increasingly large range of  $\theta$  values yields an unperturbed EPR spectrum.
- (50) G. Palmer, "Methods for Determining Metal Ion Environments in Proteins", Elsevier North Holland Press, Amsterdam, in press.
- (51) D. A. Buckingham, M. J. Gunter, and L. N. Mander, *J. Am. Chem. Soc.*, **100**, 2899 (1978).
- (52) B. Bleaney and K. D. Bowers, *Proc. R. Soc. London, Ser. A*, **214**, 451 (1952).
- (53) S. Dessens, B. R. Welch, and L. J. Wilson, unpublished results.
- (54) M. G. Simmons and L. J. Wilson, *J. Chem. Soc., Chem. Commun.*, 634 (1978).
- (55) See, for example, M. Ercinska and D. F. Wilson, *Arch. Biochem.*, **188**, 1 (1978).
- (56) W. E. Blumberg and J. Peisach, *Biophys. J.*, **25**, 34a (1979).
- (57) W. Blumberg, The Japanese-American Seminar on Cytochrome Oxidase, Kobe, Japan, 1978, Paper 27.
- (58) C. A. Reed and J. T. Landrum, *FEBS Lett.*, in press.
- (59) P. D. W. Boyd and T. D. Smith, *Inorg. Chem.*, **10**, 2041 (1971); M. Nicholas, R. Mustaceich, and D. Jayne, *J. Am. Chem. Soc.*, **94**, 4518 (1972). For other FeOFe systems see D. H. O'Keefe, C. H. Barlow, W. S. Caughey, G. A. Smythe, W. H. Fuchsman, T. H. Moss, and H. R. Lilienthal, *Bioinorg. Chem.*, **5**, 125 (1975).
- (60) B. Chance, C. Saronio, and J. S. Leigh, *Proc. Natl. Acad. Sci. U.S.A.*, **72**, 1635 (1975).
- (61) See, for example, E. Bayer, D. Krauss, A. Roder, and D. Schretzmann, "Oxidases and Related Redox Systems", Vol. I, T. E. Kline, H. S. Mason, and M. Morrison, Eds., University Park Press, Baltimore, Md., 1973, Chapter II.
- (62) See, for example, J. V. Bannister, Ed., "Structure and Function of Haemocyanin", Springer-Verlag, West Berlin, 1977.
- (63) K. M. Kadish, G. Larson, D. Lexa, and M. Momenteau, *J. Am. Chem. Soc.*, **97**, 282 (1975).

## Volatility and Molecular Structure of Neptunium(IV) Borohydride

Rodney H. Banks, Norman M. Edelstein,\* Brock Spencer,<sup>1</sup> David H. Templeton,\* and Allan Zalkin\*

Contribution from the Materials and Molecular Research Division, Lawrence Berkeley Laboratory, and Department of Chemistry, University of California, Berkeley, California 94720. Received June 27, 1979

**Abstract:** The structure of  $\text{Np}(\text{BH}_4)_4$  was determined by single-crystal X-ray diffraction methods at 130 K. The crystals are tetragonal, space group  $P4_2/nmc$ ;  $a = 8.559(9) \text{ \AA}$ ,  $c = 6.017(9) \text{ \AA}$ ,  $Z = 2$ .  $R = 0.114$  for 352 reflections (Mo  $K\alpha$  radiation). The four borohydride ions are disposed tetrahedrally about the Np with Np-B distances of  $2.46(3) \text{ \AA}$ . The boron atoms are connected to the Np atom with triple hydrogen bridge bonds similar to the terminal borohydrides in uranium borohydride. Hydrogen atoms were observed in the Fourier maps and refined. This molecular structure is similar to that found for hafnium and zirconium borohydride, but the space group is different. The vapor pressure, 10 mmHg at  $25^\circ\text{C}$ , was measured in the range of  $-5$  to  $25^\circ\text{C}$  using a Bourdon gauge.

### Introduction

The relationship between the physical properties and structures of metal borohydrides has been studied extensively since the first preparation of metal compounds containing the  $\text{BH}_4^-$  anion.<sup>2</sup> One property which has attracted attention is the high volatility exhibited by some of them.<sup>3,4</sup> No univalent metal borohydride is volatile and only a few of the lighter bis- and trisborohydrides show volatility below room temperature.<sup>5</sup> Tetravalent Th, Pa, and U form borohydrides of low volatility, while Zr, Hf, Np, and Pu give tetrakisborohydrides of greater volatility.

The crystal structures of these seven compounds fall into three types. Thorium,<sup>3a</sup> protactinium,<sup>4</sup> and uranium<sup>6,7</sup> borohydrides show one structure type which has been studied by X-ray and neutron diffraction methods for  $\text{U}(\text{BH}_4)_4$ . The 14-coordinate uranium is surrounded by six  $\text{BH}_4^-$  groups, two of which are triply hydrogen bridge bonded to the metal with a U-B distance of  $2.53 \text{ \AA}$ . The other four borohydride groups are bonded to the uranium by double hydrogen bridges giving a longer U-B distance of  $2.87 \text{ \AA}$ . These four bridging  $\text{BH}_4^-$  units use their remaining two hydrogens to link adjacent U atoms in a polymeric structure of  $C_2$  symmetry at uranium.

Neutron-diffraction results on  $\text{Hf}(\text{BH}_4)_4$ <sup>8</sup> and an X-ray diffraction study on the isostructural  $\text{Zr}(\text{BH}_4)_4$ <sup>9</sup> have shown that these molecules crystallize into a different structure type and are monomeric. The metal atom is bonded to four tetrahedrally arranged borohydride groups by triple hydrogen bridge bonds giving the molecule rigorous  $T_d$  symmetry. The coordination sphere around Zr or Hf consists of only 12 hydrogen atoms. The corresponding Zr-B and Hf-B distances are  $2.34(3)$  and  $2.28(1) \text{ \AA}$ , respectively.<sup>8a,9</sup>

The third type,<sup>4</sup> displayed by  $\text{Np}(\text{BH}_4)_4$  and  $\text{Pu}(\text{BH}_4)_4$ , is somewhat similar to that of zirconium and hafnium borohydrides and is discussed here in detail.

In order to put the volatility of the third structure type on a quantitative basis, vapor-pressure measurements of  $\text{Np}(\text{BH}_4)_4$  were carried out as a function of temperature, yielding various thermodynamic quantities. An X-ray crystallographic investigation of  $\text{Np}(\text{BH}_4)_4$  at 130 K was undertaken to determine its detailed molecular structure.

### Experimental Section

**Vapor-Pressure Measurement.** <sup>237</sup>Np(BH<sub>4</sub>)<sub>4</sub> was prepared and purified as described previously.<sup>4</sup> The extreme chemical reactivity of  $\text{Np}(\text{BH}_4)_4$  precluded the use of a mercury manometer and only an all-glass-and-Teflon Bourdon gauge was found satisfactory for these measurements. The exposed surfaces of the gauge were passivated with the neptunium borohydride vapor prior to use to minimize a decomposition reaction which evolves hydrogen and diborane.<sup>4</sup> Excess  $\text{Np}(\text{BH}_4)_4$  was condensed into the passivated gauge and the gauge was pumped out at  $-78^\circ\text{C}$ . At various temperatures, the compound was allowed to vaporize and deflect a pointer, whose initial position was precisely determined by a cathetometer. Shortly after equilibrium was established, the pointer was nulled to its original position by pressurizing the outer chamber of the gauge with argon. The argon pressure, as measured by a standard pressure gauge, then equaled the vapor pressure of the  $\text{Np}(\text{BH}_4)_4$ . Care was taken to remove all traces of  $\text{H}_2$  and  $\text{B}_2\text{H}_6$  before and after each measurement. Vapor-pressure readings were taken at room temperature and below until the vapor pressure of the compound approached the sensitivity of the Bourdon gauge.

**Crystal Preparation.** A sample of the dark green liquid  $\text{Np}(\text{BH}_4)_4$  was sealed into a 0.3 mm i.d. quartz capillary and stored in liquid nitrogen prior to use. The capillary was mounted on a Picker FACS-I